Journal of Applied Polymer Science

A Novel Approach to Prepare Etoposide-Loaded Poly(*N*-Vinyl caprolactam-*co*-methylmethacrylate) Copolymeric Nanoparticles and Their Controlled Release Studies

Sunil Shah,[1,2] Angshuman Pal,[2] Rajiv Gude,[3] Surekha Devi[2]

[1]Shah-Schulman Center for Surface Science and Nanotechnology, Faculty of Technology, Dharmsinh Desai University, Nadiad, Gujarat, India

[2]Department of Chemistry, Faculty of Science, The Maharaja Sayajirao University of Baroda, Vadodara, 390002, India

[3]Gude Lab, Cancer Research Institute, Advanced Centre for Treatment Research and Education in Cancer (ACTREC), Tata Memorial Centre, Kharghar, Navi Mumbai, 410210, India

Correspondence to: S. Shah (E-mail: sunil.sscssn@ddu.ac.in)

ABSTRACT: A series of copolymeric nanoparticles of methyl methacrylate and *N*-vinylcaprolactam were synthesized from microemulsions containing sodium dodecyl sulfate. Etoposide as a model drug was loaded in nanoparticles during *in situ* polymerization. Stable nanolatex were produced and characterized for size and shape by dynamic light scattering (DLS) and transmission electron microscopy. Particles were found to be spherical in nature with size less than 50 nm. Structural characterization of copolymers was done by infrared and nuclear magnetic resonance spectroscopy. Differential scanning calorimetery (DSC) and X-ray diffractometry (XRD) techniques were used to evaluate molecular level interaction of etoposide with nanoparticles. Drug encapsulation efficiency was determined by ultraviolet (UV) spectrometry and found to be 35–67%. DSC, XRD, and UV data suggested the molecular level dispersion of drug in the nanoparticles. *In vitro* release studies and *in vitro* cytotoxicity showed prolonged and controlled release of etoposide from nanoparticles along with IC_{50} values of nanoparticles in the range of 0.01–0.1 mg/mL. © 2012 Wiley Periodicals, Inc. J. Appl. Polym. Sci. 000: 000–000, 2012

KEYWORDS: nanoparticles; etoposide; microemulsion polymerization; B16F10; melanoma cell lines; cytotoxicity

Received 5 January 2012; accepted 20 May 2012; published online
DOI: 10.1002/app.38107

INTRODUCTION

Podophyllotoxin is an antimitotic natural product and its inhibitory action on cell growth led to expansion of the clinically important anticancer agents, etoposide and teniposide. The cytotoxic mechanism of these drugs is the inhibition of topoisomerase II. It has been used in the treatment of a variety of malignancies like malignant lymphoma, brain stem gliomas, small cell lung carcinoma, stomach cancer, and ovarian cancer. Among them, etoposide, a semisynthetic epipodophyllotoxin derivative, is a first choice drug for the treatment of the above mentioned diseases.[1–3] However, its degradation at pH 1.3; poor water solubility and slow intrinsic dissolution rate make it quite challenging to prepare optimal formulation from it.[4,5] Several investigational oral formulations of etoposide had been developed but all suffered the disadvantage of low and erratic bioavailability.[6] Hence, efforts were made to boost the bioavailability of the drug. The presently existing commercial oral formulations are nonaqueous, that is, parenteral solutions and oral soft gelatin capsules containing etoposide solution in a mixed solvent system comprising benzyl alcohol, ethanol, PEG 400, and Tween 80.[7–9] However, both of these formulations have disadvantages. Etoposide precipitates from the parenteral solution when diluted with other intravenous fluids, and conversely, the oral soft gelatin capsule formulations exhibited low bioavailability.[10]

Attempts have been made to increase the water solubility of etoposide through chemical modification, that is, prodrug, such as etoposide phosphate. However, it has not yet proved whether this path can actually improve oral bioavailability. Shah et al.[5] implement another approach by disturbing the crystalline nature to increase the water solubility and dissolution rate of the drug by solid state dispersion of drug into water soluble carrier molecules, which significantly reduces the crystallinity of drug. They have reported two times increase in the solubility and 42 times increase in dissolution rate leading to increase in the oral bioavailability of etoposide. Recently, due to emergence of

genomic era, new drug targets have been identified, because of which controlled release (CR) and targeted drug delivery systems have become popular research areas. A recent trend has been the use of particulate drug delivery technology, where the payload (hydrophilic and hydrophobic drugs) is trapped within the carrier system of 1–1000 nm in diameter. Nanocarriers, due to their multifaceted specific properties like effective targeting of hydrophilic as well as hydrophobic drugs at the site of action, long shelf-life and high encapsulation efficiency of drugs unlike liposomes often exhibit similarity in their size and structure to natural carriers such as viruses and serum lipoproteins.[11–13]

In the search of an ideal system, a number of carrier systems have appeared in the literature on formulation of nanodispersions for controlled delivery of bimolecules/drugs.[14–20] Basically, nanodispersion is reported to be prepared by top-down approach or bottom-up approach.[21] In top-down approach, the particulate size is reduced by either providing external forces such as sonication, high pressure homogenization, or dispersion of preformed polymer by means of organic solvents, which can be hazardous to the biological environment. In bottom-up approach, *in situ* polymerization technique is used where it has been found that drug can be combined with nanoparticles through dissolution in the polymerization medium, either before the introduction of the monomer or after polymerization. Development of smaller sized particles with high specific surface area with porous nature and spherical morphology enables a large variety of entrapped drugs to be successfully delivered at different parts of body. For instance, Xu et al.[22] synthesized effective core-surface crosslinked nanoparticulate drug delivery vehicle for cisplatin. Babu et al.[23] performed polymerization of acrylamide and methyl methacrylate (MMA) to produce novel core–shell microspheres and investigated the release of anticancer agent 5-fluorouracil entrapped through absorption, adsorption technique in the presence of crosslinking agent. An improved release profile with a higher entrapment of drug was reported for a 3 : 1 ratio of acrylamide to MMA core–shell microparticles prepared by an *in situ* polymerization method.

Recently, poly(*N*-vinylcaprolactam) (PVCL) water soluble, biodegradable, temperature responsive polymer having lower critical solution temperature near to body temperature (around 32°C) has attracted much attention of researchers and technologist.[24] So far, only a few studies related to its properties and applications have been reported even though PVCL has been commercially available from Badische Anilin- und Soda-Fabrik (BASF) for a long period of time. Much of the published work is concentrated on the PVCL-based hydrogels as they have potential applications in controlled drug delivery system, separation science, immobilization of enzymes, and tertiary oil-recovery technology.[25–29] Similarly, colloidal systems can be equally attractive for such applications, which could be easily synthesized through free radical microemulsion polymerizations. Pelton and Chibante[30] reported first time in 1986 synthesis of temperature sensitive microgel from *N*-isopropylacrylamide (NIPAM) and *N,N′*-methylene bisacrylamide as a crosslinker. After that, many research papers were published on copolymeric microgels based on NIPAM and other ionic monomers.

As a part of our ongoing research on the development of novel CR systems,[31–33] attempts are made to synthesize temperature responsive copolymeric nanoparticles through microemulsion copolymerization of MMA and *N*-vinyl caprolactam (VCL) of different compositions for the entrapment of high molecular weight lipophilic model drug etoposide and for the investigation of its release pattern. The nanoparticles formed are characterized by dynamic light scattering (DLS), transmission electron microscopy (TEM), differential scanning calorimetry, X-ray diffractometry, and infrared (IR) spectrometry. Entrapment efficiency and *in vitro* release of etoposide from nanoparticles was also studied. To our knowledge, these copolymeric nanoparticles are not reported so far in the literature and their use for loading of etoposide is reported for the first time. Attempts are made to find out the possible cytotoxicity effect of etoposide-loaded nanoparticles on B16F10 melanoma cancer cells.

EXPERIMENTAL

Materials

Etoposide (99.9%) was obtained as a gift sample from Cipla, Mumbai, India. VCL, (98%, Sigma-Aldrich, Steinheim, Germany) and MMA (Merck, Mumbai, India) were distilled under high vacuum and stored at 4°C before use. L-Ascorbic acid, hydrogen peroxide (30% w/v, Merck, Mumbai, India) and sodium dodecyl sulfate (SDS) from SD-Fine Chem., Baroda, India were used as received. Double distilled deionised water (0.22 μm nylon filtered) was used throughout the experiments.

Cell Culture

B16F10, a highly metastatic lung selected subline derived from C57/BL6 murine melanoma, was purchased from National Centre for Cell Science (Pune, India). The cell line was maintained as a continuous culture in Iscove's minimum Dulbecco's medium (GIBCO, BRL, MD) supplemented with 10% fetal bovine serum (GIBCO BRL), 100 units/mL penicillin and 100 μg/mL streptomycin. Cells were grown in a humidified atmosphere of 5% CO_2 and 95% air at 37°C. Media was replenished every third day.

Synthesis of Copolymeric Nanoparticles and Etoposide-Loaded Copolymeric Nanoparticles

Copolymeric nanoparticles of various compositions with and without etoposide were prepared by without microemulsion polymerization technique. The ternary microemulsions comprising MMA-VCL monomer mixture having monomer weight ratios varying from 100 : 0 to 25 : 75 MMA : VCL, SDS (2%, w/w) and water (91%, w/w) were taken in three-neck reaction vessel equipped with a nitrogen inlet, thermometer, water condenser, and magnetic stirrer. Typically, monomer to surfactant ratio was kept constant at 3 for all recipes. The ternary microemulsion was deoxygenated by bubbling purified nitrogen for 15 min. Polymerization was initiated by redox initiator pair hydrogen peroxide and L-ascorbic acid at 40 ± 2°C. MMA was added drop wise to maintain the monomer ratio in feed.[33,34] The nanolatex obtained after completion of the reaction was purified by centrifugation at 5000 rpm at Krafft temperature (16°C) of surfactant to achieve surfactant free nanolatex and it was further lyophilized using Heto Dry winner, Germany to separate nanoparticles. The adsorbed surfactant was removed by redispersing

lyophilized drug loaded nanoparticles in hot water and then centrifuging the suspension at 5000 rpm for 30 min at 16°C thrice. Lyophilization was done after removal of supernatant to obtain the dry nanoparticles for further structural characterization. Monomer mixture containing 1% (w/w) etoposide and the above synthesis procedure was followed for preparation of etoposide-loaded nanoparticles.

Characterization

Spectroscopic Analysis. The IR spectra of the purified copolymer, drug loaded copolymer and drug was recorded on a Perkin Elmer Rx_1 IR spectrophotometer (MA) using 1-cm diameter KBr pellets. ^{1}H NMR spectrum of placebo copolymeric nanoparticles was recorded using 400 MHz ^{1}H NMR spectrometer (Bruker specrospin Avance Ultra-shield, Germany) at room temperature ($\sim$ 30 $\pm$ 2°C). The spectrum was obtained after accumulating 16 scans using 1% sample in $CDCl_3$.

Differential Scanning Calorimetry. Differential scanning calorimetric (DSC) analysis of the placebo poly(MMA-*co*-VCL) copolymeric nanoparticles (50 : 50), etoposide-loaded copolymeric nanoparticles, etoposide and physical mixture of etoposide and copolymeric nanoparticles (1 : 1 w/w) was performed using a Mettler–Toledo 822 instrument (Greifensee, Switzerland). The instrument was calibrated using indium as a standard and samples were heated in sealed aluminum pans between 0 to 400°C at a heating rate of 10°C min^{-1}.

Powder X-ray Diffraction. Powder X-ray diffraction (XRD) patterns of the placebo (MMA-*co*-VCL) copolymeric nanoparticles (50 : 50), etoposide-loaded copolymeric nanoparticles, etoposide, and physical mixture of etoposide and copolymeric nanoparticles (1 : 1) were recorded on a Philips X'pert (MPD range, Germany) using a Ni-filtered Cu Kα radiation (1.5405 A°) over the 2θ range of 3–100°.

Dynamic Light Scattering. A Brookhaven's 90 plus DLS equipment (Holtsville) with a 30-mW solid state laser source operated at 688 nm was used to measure the particle size and size distribution of the polymerized latex in a dynamic mode. The particle size was obtained from the Stokes–Einstein relation

$$D = kBT/(6\pi\eta d) \quad (1)$$

where d is the diameter of particles, D is the translational diffusion coefficient, k is the Boltzmann constant, T is the temperature (°C), and η is the viscosity (centipoises) of the medium. The scattering intensities from the samples were measured at 90° using photomultiplier tube. To minimize the interparticle interactions, the analysis of the latex was done after 10 times dilution considering the refractive index and viscosity of water as that of latex. All the measurements were performed in triplicate and mean values were taken.

Transmission Electron Microscopy. TEM analysis of copolymeric nanoparticles and etoposide-loaded copolymeric nanoparticles was performed using JEOL 1200 EX Transmission Electron Microscope at accelerating voltage of 80 kV. One drop of latex was dispersed in 5 mL of water and was placed on the carbon-coated copper grid. The grid was dried under IR lamp and then the images of representative areas were captured at suitable magnifications.

Gel Permeation Chromatography. Molecular weights of copolymers were determined after lyophilization of the latex using Perkin Elmer Totalchrom instrument with turbosec size exclusion software equipped with a PE-series 200 RI detector, series 200 isocratic pump, and rheodyne injector. The PLGel 5 μm mixed column, suitable for molecular weights up to 10^4–10^7 was used in polar solvent. Distilled, degassed tetrahdrofuran (THF) at flow rate of 1 mL/min was used as an eluent. Medium molecular weight polystyrene standards (POLYSCI, 1 mg/mL in THF, with molecular weights 1×10^3–3×10^5) were used for calibration of gel permeation chromatography (GPC).

Estimation of Percentage Encapsulation Efficiency. The ultraviolet (UV) spectra of the purified copolymer, etoposide, and etoposide-loaded copolymers were recorded on a Perkin Elmer Lambda 35 UV/Vis Spectrophotometer. The drug loaded nanoparticles were purified by successive washing with methanol to remove the adsorbed drug and then relyophilized. Ten milligrams of nanoparticles were dissolved in 10 mL of chloroform. Entrapment efficiency of etoposide in nanoparticles was calculated from the calibration plot constructed at 293 nm after confirming the noninterference of polymers in the absorption region of etoposide. All measurements were performed in triplicate and the average values were considered.

***In vitro* Release.** *In vitro* release study for etoposide-loaded copolymeric nanoparticles of various compositions was performed in a dialysis bag (cutoff 10,000, Hi-Media, Mumbai, India) diffusion technique.[35] Etoposide release from the nanoparticles was studied in phosphate buffer of pH 7.4 containing 0.1% Tween 80 at room temperature (30$\pm$ 2°C). The aqueous nanoparticulate dispersion equivalent to 1 mg etoposide was placed in cellulose dialysis bag and sealed at both ends. The dialysis bag was immersed in the receptor compartment containing 50 mL of the dissolution medium and stirred at 100 rpm under magnetic stirring. Aliquots of samples were withdrawn at regular time intervals and the same volume was replaced with fresh dissolution medium. The samples were analyzed by UV spectrophotometer at 293 nm against reagent blank. All experiments were repeated thrice and the average values were considered.

Cytotoxicity Assay. Cytotoxicity of the etoposide-loaded copolymeric nanoparticles was evaluated using B16F10 cell lines. Cells were seeded in 96-well microplates at a density of 5×10^3 cells/well. Cells were allowed to grow and stabilize for 24 h. They were then treated with different concentrations of different compositions of etoposide-loaded poly(MMA-*co*-VCL) copolymeric nanoparticles for 24 h, to find their cytotoxic effect. The prepared nanoparticles being assayed were added directly to the medium in each well at the dilutions 0.00001–0.5 mg/mL. On each 96-well plates, four wells were left untreated for use in calculating the 100% optical density (OD) values. Post-treatment cell viability was determined by 3-(4,5-dimethyl-2-thiazolyl)-2,5-diphenyltetrazolium bromide (MTT) colorimetric assay. MTT reagent (Sigma-Aldrich) was added to each well to make a final concentration of 1 mg/mL of media and incubated for 4 h

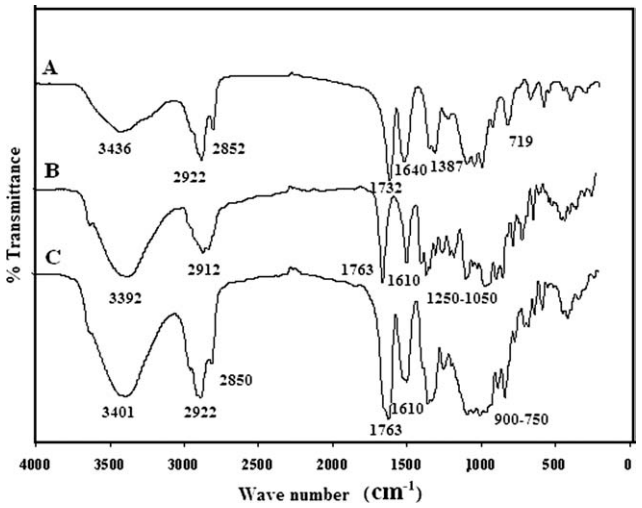

Figure 1. FTIR spectra of (A) poly (MMA-*co*-VCL) copolymer, (B) etoposide, and (C) etoposide-loaded copolymeric nanoparticles.

at 37°C. Formazan crystals were dissolved in 100 μL of dimethyl sulfoxide (DMSO); the OD was measured in the enzyme-linked immunosorbent assay plate reader (Molecular Devices, Spectra Max 190 with Soft max Pro) at 540 nm with a reference wavelength of 690 nm.

RESULT AND DISCUSSION

FTIR Analysis

FTIR spectra of copolymeric nanoparticles, pure etoposide, and etoposide-loaded copolymeric nanoparticles were recorded and are given in Figure 1. The carbonyl stretching vibrations of the MMA and VCL units of the copolymer [Figure 1(a)] appear as a very strong absorption bands at 1732 and 1640 cm^{-1}, respectively. The copolymer being hydrogel in nature, the appearance of a strong but broadband at 3436 cm^{-1} can be attributed to the presence of water of hydration in copolymer. Krish et al.[36] studied detailed structural transformations and interactions of PVCL and water using various methods such as IR-spectroscopy, quantum-chemical calculations, DSC, and optical microscopy and have reported that PVCL macromolecules in aqueous solution are the highly modified water associated structures, being affected by the polarization action of highly polar amide groups due to specific configurational and conformational structures of the polymer. The bands appearing at 2922, 2852, 1447, and 1387 cm^{-1} are attributed to stretching and bending vibrations of $>CH_2$, $>CH-$ groups respectively. Bands appearing at 1045 cm^{-1}, 1245 cm^{-1} correspond to ester stretching vibration of acrylate polymer and bands appearing at 719 cm^{-1} correspond to the presence of more than three $>CH_2$ groups in a cyclic structure, providing evidence of copolymerization. IR spectrum of etoposide [Figure 1(b)] exhibits, strong absorption peaks at 3392, 2912, 1763 −1610, 1500–1300, 1250–1050, and 950–850 cm^{-1} corresponding to —OH, —CH_2 stretching, lactone group, ring stretching, C—O—C linkages and substituted ring stretching, respectively, as reported earlier. Although in the case of etoposide-loaded copolymeric nanoparticles [Figure 1(C)], presence of characteristics bands of drug and copolymer at 3401, 2922, 2852, 1763–1610, 1520–1300, 1250–1050, and 900–750 cm^{-1} correspond to —OH, $>CH_2$ stretching, lactone group, ring stretching, C—O—C linkages and the presence of more than three —CH_2 groups in cyclic structure supporting

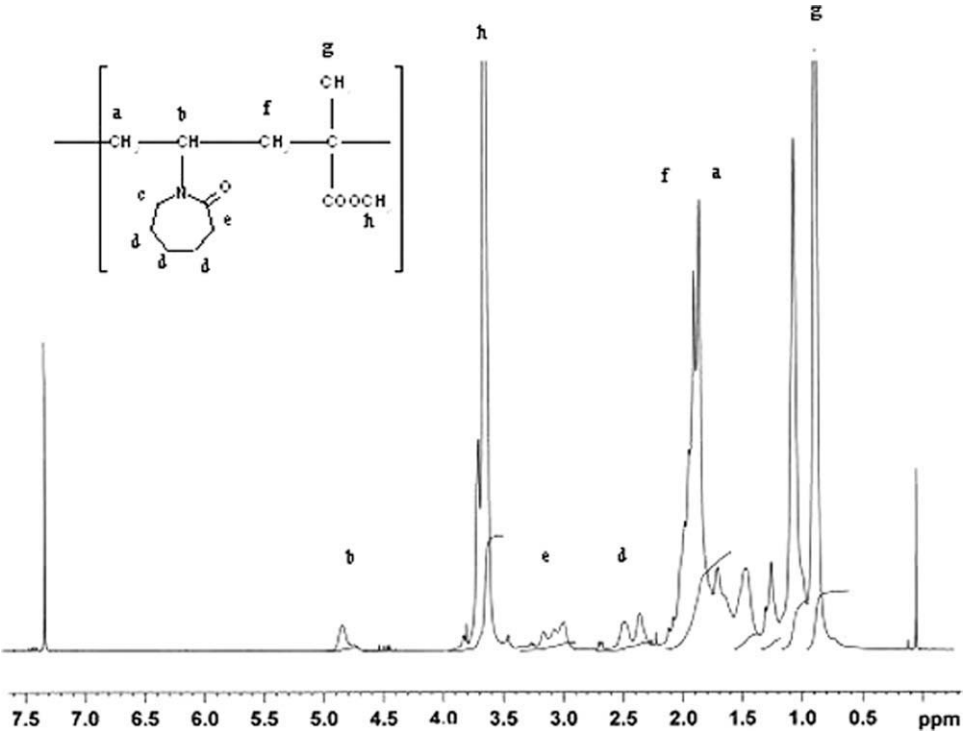

Figure 2. ^{1}H NMR spectrum of 50 : 50 poly (MMA-*co*-VCL) copolymer.

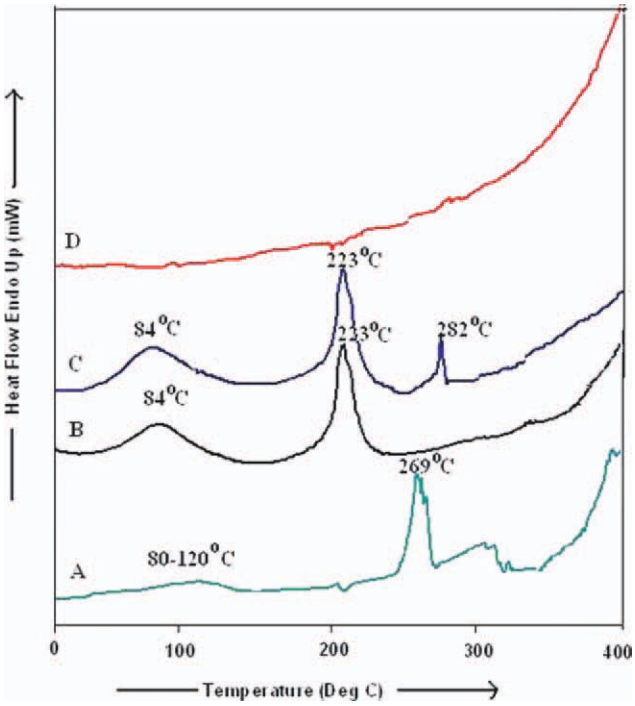

Figure 3. DSC thermograms of (A) etoposide, (B) poly (MMA-*co*-VCL) copolymeric nanoparticles (50 : 50), (C) physical mixture of etoposide and copolymeric nanoparticles (1 : 1 w/w), and (D) etoposide-loaded copolymeric nanoparticles. [Color figure can be viewed in the online issue, which is available at wileyonlinelibrary.com.]

the existence of etoposide in nanoparticles.[36] Changes observed in FTIR spectrum of the etoposide-loaded copolymer might be due to the interaction between drug and polymer or difference in the polymer morphology due to the presence of small quantity of etoposide.[37–39]

Nuclear Magnetic Resonance Spectroscopy

A representative ^{1}H NMR spectrum of 50 : 50 poly (MMA-*co*-VCL) copolymer is given in Figure 2. The composition of the copolymer was determined by linear and nonlinear least square methods[34] from the well separated signals that appeared at 4.798 ppm corresponding to the proton from a caprolactam ring of the VCL units and the signal that appeared near 0.84–1.1 ppm corresponding to the methyl proton of the MMA units. This also provides evidence for copolymerization.[40,41]

Differential Scanning Calorimetry

DSC thermograms of (A) etoposide, (B) copolymeric nanoparticles, (C) physical mixture of etoposide and copolymeric nanoparticles, and (D) etoposide-loaded copolymeric nanoparticles are given in Figure 3. DSC thermogram of pure etoposide evidenced an endotherm over the range of 80–120°C due to dehydration of water molecules and endothermic peak at 269°C for melting followed by decomposition observed above 290°C. A similar observation is reported by Jasi et al.[40] Although endothermic peaks at 84 and 223°C are observed for lyophilized 50 : 50 poly (MMA-*co*-VCL) copolymeric nanoparticles. However, no characteristic endothermic peaks at 84°C and 269°C corresponding to copolymer and etoposide were observed in DSC plot of the etoposide-loaded copolymeric nanoparticles (D) might be due to low loading of drug in copolymer structure along with strong interaction of drug with copolymer, but two separate peaks at 84°C and 282°C corresponds to copolymeric nanoparticles and etoposide were observed in a physical mixture of copolymeric nanoparticles and etoposide (C) Similar observation was reported earlier by Babu et al.[23] From these results, we can also say the presence of possible interaction takes place between drug and polymers.

Powder X-ray Diffraction

Powder X-ray diffraction (XRD) patterns for the (A) etoposide, (B) physical mixture of etoposide and copolymeric nanoparticles (1 : 1 w/w) (C) copolymeric nanoparticles, and (D) etoposide-loaded copolymeric nanoparticles are given in Figure 4. The peaks of interest for pure drug observed at 4.2, 9.46, 10.22, 13.18, 16.15, 17.08, 17.67, 19.26, 19.89, 22.14, 23.03, 23.67, 24.17, and 26.78; indicate highly crystalline nature of the drug. Although for etoposide-loaded copolymeric nanoparticles, all the crystalline peaks of drug disappear, as only 1% of drug is present in the sample that contains etoposide in the polymer matrix. These results are in agreements with the earlier published work.[22]

Determination of Particle Size and Molecular Weight

Particle size of the etoposide-loaded copolymeric nanoparticles was determined through DLS technique and TEM (Figures 5 and 6). The particle size histograms obtained through DLS for homopolymer [polymethyl methacrylate (PMMA)], and 75 : 25, 50 : 50, and 25 : 75 poly (MMA-*co*-VCL) copolymers are shown in Figure 5(A–D) and data for etoposide-loaded copolymeric

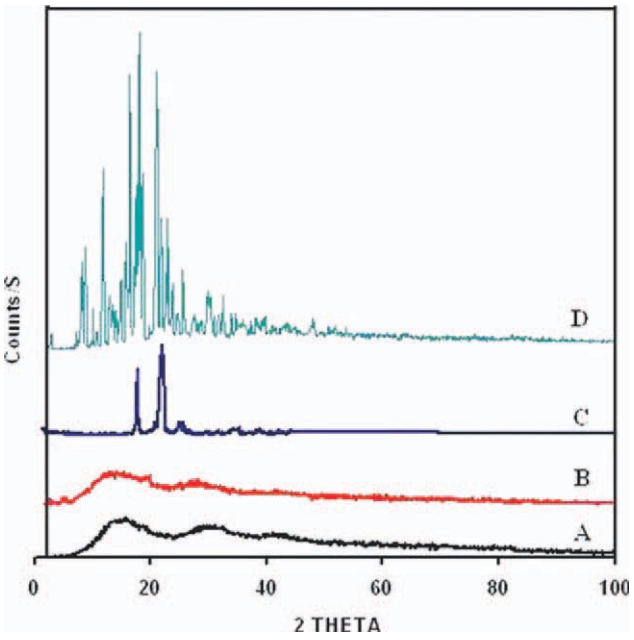

Figure 4. X-ray diffraction patterns of (D) etoposide, (C) physical mixture of etoposide and copolymeric nanoparticles (1 : 1 w/w), (B) poly (MMA-*co*-VCL) copolymeric nanoparticles (50 : 50), and (A) etoposide-loaded copolymeric nanoparticles. [Color figure can be viewed in the online issue, which is available at wileyonlinelibrary.com.]

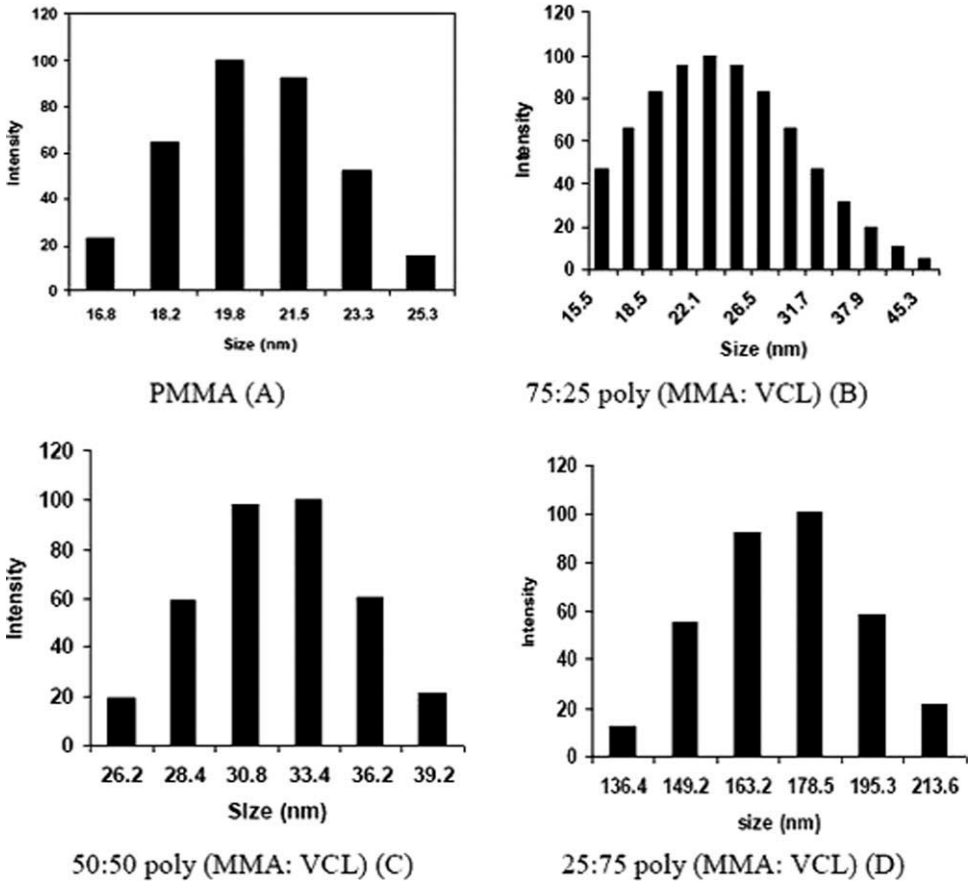

Figure 5. A representative DLS histograms of (A) PMMA, (B) 75 : 25 poly(MMA-*co*-VCL), (C) 50 : 50 poly(MMA-*co*-VCL), and (D) 25 : 75 poly (MMA-*co*-VCL) copolymers.

nanoparticles for all compositions are compiled in Table I. The particle size and polydispersity index were observed to be in the range of 20–120 nm; 0.029–0.223 and increased with increase in VCL content in the copolymer. TEM was used to examine size and morphology of etoposide-loaded copolymeric nanoparticles. Figure 6 shows TEM images of [Figure 6(A)] etoposide-loaded poly(MMA-*co*-VCL) copolymeric nanoparticles and [Figure 6(B)] placebo nanoparticles. Particles were observed to be

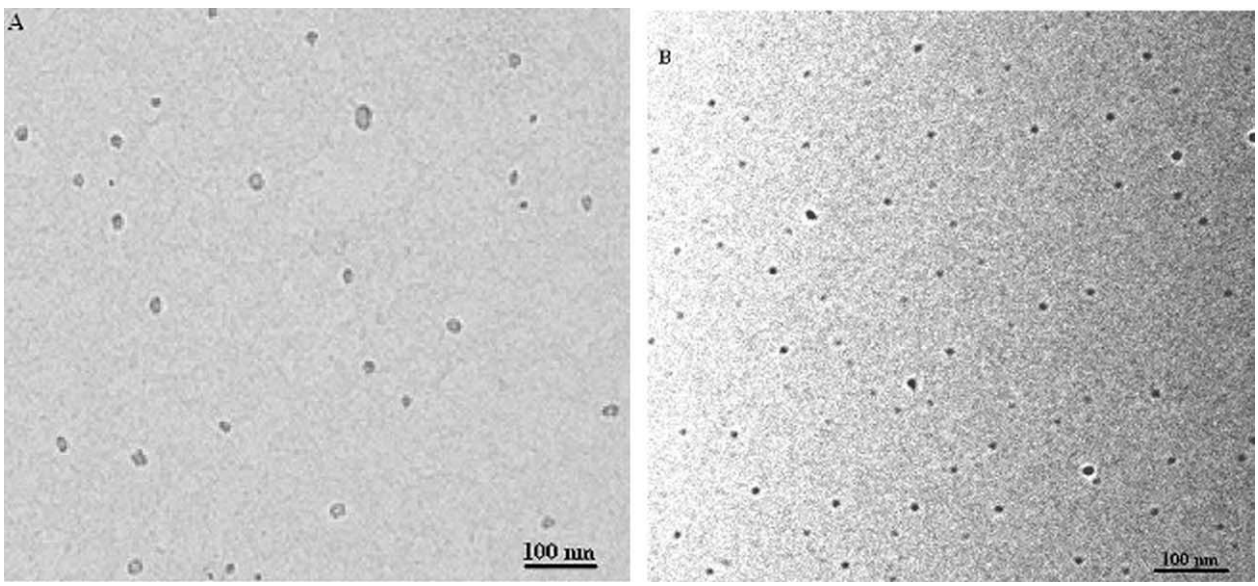

Figure 6. TEM images of (A) poly(MMA-*co*-VCL) copolymeric nanoparticles and (B) etoposide-loaded poly(MMA-*co*-VCL) copolymeric nanoparticles.

Table I. Particle Size, Molecular Weight Distribution, and Encapsulation Efficiency of Etoposide in Copolymeric Nanoparticles

Copolymer (MMA : VCL)	Particle size (nm)	PDI (DLS)	$M_w \times 10^{-4}$	$M_n \times 10^{-4}$	PDI (GPC)	Encapsulation efficiency (%)
PMMA	20 ± 1.6	0.029	1.58	1.52	1.05	67.33
75 : 25	22 ± 1.1	0.102	0.829	0.737	1.16	44.77
50 : 50	33 ± 2.4	0.132	0.745	0.600	1.24	40.43
25 : 75	178 ± 4.1	0.223	0.482	0.36	1.33	35.05

smaller than 50 nm diameters and for both placebo and etoposide-loaded nanoparticles with spherical morphology and monodispersed nature. Gel permeation chromatographic analysis of the etoposide-loaded copolymeric nanoparticles shows that molecular weight decreases and polydispersity index increases with increase in VCL content in copolymer at a fixed drug concentration (Table I). Peak molecular weight and polydispersity were found to be 1.15–0.48 $\times$ 10^5 and 1.05–1.33, respectively. These results are in good agreement with DLS data and indicate that particles are monodispersed in nature. The systematic decrease in molecular weight may be due to the exclusive polymerization of MMA during polymerization.

Entrapment Efficiency of Etoposide in Nanoparticles

The entrapment efficiency of etoposide in copolymeric nanoparticles was determined using UV-Visible spectrometry (Figure 7). The entrapment efficiency was found to vary from 35 to 68% when 1% (w/w) etoposide was added during polymerization of different monomer compositions. UV-spectrum of pure etoposide [Figure 7(A)] showed maximum absorbance (λ_{max}) around 293 nm in chloroform, whereas UV-spectrum of placebo nanoparticles did not show any peak in the UV–visible region [Figure 7(B)]. UV-spectrum of etoposide-loaded copolymeric nanoparticles [Figure 7(C_{1-4})] shows that peaks corresponding to etoposide show small red shift and exhibited maximum absorption at 296 nm. From the calibration plot at 293 nm, entrapment efficiency of etoposide in nanoparticles was calculated. Maximum entrapment efficiency (67%) of etoposide was observed for homopolymer (PMMA). Table I shows the results of entrapment efficiency of etoposide in nanoparticles of different compositions. It was observed that with increase in the VCL content in copolymerization recipe, encapsulation efficiency of etoposide decreases. This may be due to the highly hydrophobic nature of etoposide in the nanoparticle matrix and monomer partitioning effect observed during micellar polymerization. The entrapment efficiency of etoposide was also observed to be higher for smaller size particles.

In Vitro Release

The release of etoposide from copolymeric nanoparticles in phosphate buffer of pH 7.4 containing 0.1% Tween 80 is illustrated in Figure 8. The release profile of etoposide from nanoparticles was observed to be biphasic. The first phase shows initial high rate of release for maximum period of 60 min followed by the slow release phase. The total percentage cumulative release was up to the maximum of 82% for the batches with 25 : 75 poly (MMA : VCL) and the minimum of 63% for PMMA for a period of 30 h indicating a sign of CR of etoposide. The initial fast release of drug is the outcome of burst release due to the fast dissolution and quick diffusion of drug particles migrated to the periphery during the formation of the

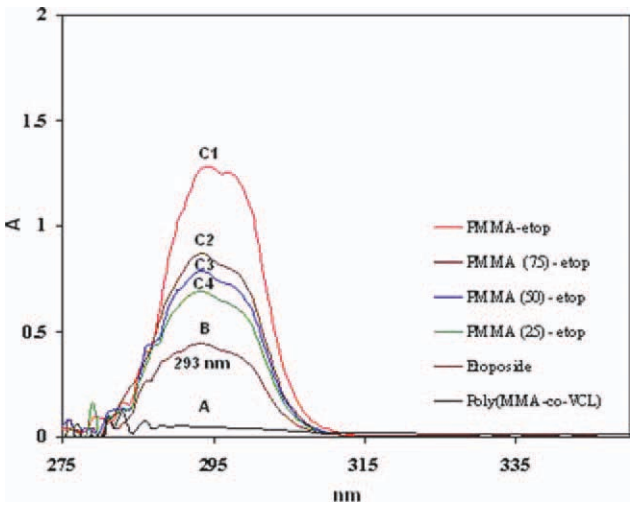

Figure 7. UVspectra of (A) etoposide, (B) copolymeric nanoparticles, and (C1-4) etoposide-loaded copolymer nanoparticles. [Color figure can be viewed in the online issue, which is available at wileyonlinelibrary.com.]

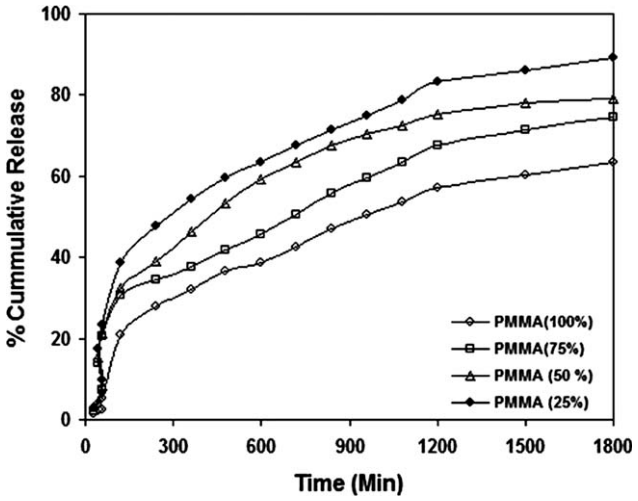

Figure 8. Percentage cumulative release pattern of etoposide through copolymeric nanoparticles. Symbols: PMMA (○), 75 : 25 Poly(MMA: VCL) (□), 50 : 50 Poly(MMA: VCL) (△), (●) 25 : 75 Poly(MMA: VCL) nanoparticles.

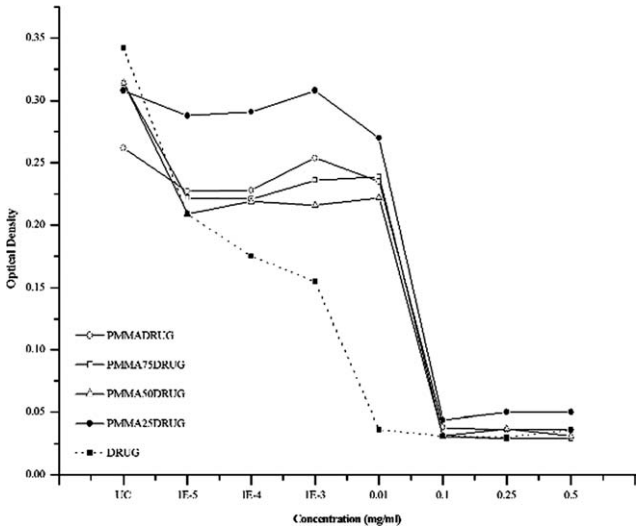

Figure 9. *In vitro* cytotoxicity profile of different composition of etoposide-loaded nanoparticles and etoposide as a control, tested in B16F10 cell lines.

particles. A drug-like etoposide has low partition coefficient (1.7) at acidic pH and diffuses faster in the hydrophilic polymer matrix than in a hydrophobic polymer matrix. A similar observation is seen in the present case where polymers with higher hydrophobic character (100% PMMA) show lower burst release of etoposide (∼ 5%) with respect to low hydrophobic (25% PMMA) nature copolymeric nanoparticles.

In Vitro Cytotoxicity

As a part of our ongoing research on the development of novel CR systems,[31–33] attempts were made to synthesize various acrylate nanoparticles for the entrapment of model drugs like acryflavin, carbamazepine, and lamotrigine for the investigation of their release patterns through emulsion and microemulsion polymerization technique. Such polymeric nanoparticles are being used for encapsulation of drugs, but very few attempts are made for biological applications of these systems. Polyacrylates are commonly used in biomedical applications; but toxicity associated with nanoparticles itself has not been systematically addressed. *In vitro* cytotoxicity effect of etoposide and etoposide-loaded poly(MMA-*co*-VCL) copolymeric nanoparticles on B16F10 cells was examined for a period of 24 h. *In vitro* cytotoxicity studies were conducted with the series of copolymeric nanoparticles against B16F10 melanoma cell lines and were reported earlier by Shah et al.[34] Figure 9 shows the cytotoxic effect of etoposide and etoposide-loaded copolymeric nanoparticles on B16F10 melanoma for a period of 24 h. Etoposide, placebo nanoparticles, and etoposide-loaded nanoparticles inhibit B16F10 melanoma cell viability. The preliminary evaluation of cell-viability data shows that, IC_{50} value of etoposide and etoposide-loaded copolymeric nanoparticles was observed to be in the range of 0.00001–0.0001 mg/mL and 0.01–0.1 mg/mL, respectively. Current clinical administration methods for etoposide have a relatively high toxicity. The synthesis of poly(MAA-*co*-VCL) nanoparticles in this study may lead to a new approach for delivery of etoposide and many other hydrophobic therapeutic agents. Using this technique, high dose of etoposide can be initially injected and etoposide will be slowly released from the nanoparticles. As etoposide will be released at a lower rate from nanoparticles, the nanoparticles minimize the systemic toxicity and reduce the number of injections necessary to maintain systematic concentrations of etoposide. This type of system can also be used for local therapy, if injected at the site of a tumor due to particle diameter which ranged from 20 to 50 nm and also a thermo responsive nature of polymer can help in the CR of etoposide at tumor site.

CONCLUSIONS

The addition of a model high molecular weight drug etoposide to copolymeric nanoparticles synthesized through microemulsion polymerization proved to be successful with a 35–67% drug entrapment with respect to copolymer compositions. The incorporation of etoposide did not appear to interfere significantly in the physicochemical properties of the polymer such as structure, molecular weight, particle size, and morphology. IR and ^{1}H NMR analysis confirmed the copolymer formation. DSC and XRD analysis indicates the molecular level dispersion of drug in polymeric matrix. TEM, DLS, and GPC analysis of nanolatex confirmed the formation of well defined reasonably well monodispersed particles with spherical morphology. As the VCL content increases in copolymer, increase in particle size and polydispersity and decrease in molecular weight and encapsulation efficiency of etoposide was observed. *In vitro* release profile of etoposide from copolymeric nanoparticles shows initial burst effect followed by continuous slow release for a period of 30 h indicating a sign of CR of etoposide from nanoparticles. Preliminary biological characterization of etoposide-loaded copolymeric nanoparticles shows possible technologically important route for etoposide-based nanoparticles formulation.

REFERENCES

1. Beijnen, J. H.; Holthuis, J. J. M.; Kerkdijk, H. G.; Vander Houwen, O. A. G. L.; Paalman, A. C. A.; Bult, A.; Underberg, W. J. M. *Ind. J. Pharm. Sci.* **1988,** *41*, 169.
2. Hande, K. R. *Eur. J. Cancer* **1998,** *34*, 1514.
3. Issell, B. F.; Crooke, S. *Cancer Treat. Rev.* **1979,** *6*, 107.
4. Shah, J. C.; Chen, J. R.; Chow, D. *Pharm. Res.* **1989,** *6*, 408.
5. Shah, J. C.; Chen, J. R.; Chow, D. *Int. J. Pharm.* **1995,** *113*, 103.
6. Clark, P. I.; Slevin, M. L. *Clin. Pharmacokinet.* **1987,** *12*, 223.
7. Gate, E. N.; Slack, J. A.; Stevens, M. F. G. Pharmaceuticals containing antitumor agents and N-methylformamide. Brit. Pat. **1984,** WO 84 01506.
8. Sato, F.; Lwasaki, M.; Ninomiya, H.; Antitumor etoposide injection. Jpn. Pat. **1984,** JP 60238415.
9. Du, J.; Vasavada, R.; *Drug Dev. Ind. Pharm.* **1993,** *19*, 903.
10. Sinkule, J. A. *Pharmacotherapy* **1984,** *4*, 61.
11. Kawashima, Y. *Adv. Drug Deliv. Rev.* **2001,** *47*, 39.

12. Gref, R.; Minamitake, Y.; Peracchia, M. T.; Trubetskoy, V.; Torchilin, V.; Langer, R. *Science* **1994,** *263*, 1600.
13. Hans, M. L.; Lowman, A. M. *Curr. Opin. Solid State Mater. Sci.* **2002,** *6*, 319.
14. Leroux, J. C.; Allemann, E.; De, J. F.; Doelker, E.; Gurny, R. J. *Controlled Release* **1996,** *39*, 339.
15. Watanabe, J.; Iwamoto, S.; Ichikawa, S. *Colloids Surf. B* **2005,** *42*, 141.
16. Radwan, M. A. *Drug Dev. Ind. Pharm.* **1995,** *21*, 2371.
17. Bajpai, A. K.; Choubey, J. *J. Appl. Polym. Sci.* **2006,** *101*, 2320.
18. Panyam, J.; Williams, D.; Dash, A.; Leslie-Pelecky, D.; Labhasetwar, V. *J. Pharm. Sci.* **2004,** *93*, 1804.
19. Alonso, M. J. In Pharmaceutical Dosage Forms; Disperse Systems; Lieberman, H., Rieger, A., Banker, M. M., Eds.; Marcel Dekker: New York, **1996,** pp 203–242.
20. Moghimi, S. M.; Hunter, A. C.; Murray, J. C. *Pharmacol. Rev.* **2001,** *53*, 283.
21. Ravi Kumar, M. N. V. *J. Pharm. Pharm. Sci.* **2000,** *3*, 234.
22. Xu, P.; Van Kirk, E. A.; Li, S.; Murdoch, W. J.; Ren, S. J.; Hussain, M. D.; Redosz, M.; Shen, Y. *Colloid Surf. B* **2006,** *48*, 50.
23. Babu, R. V.; Malladi, S.; Hosamani, K. M.; Aminabhavi, T. M. *Int. J. Pharm.* **2006,** *325*, 55–62.
24. Ballauff, M.; Lu, Y. *Polymer* **2007,** *48*, 1815.
25. Das, M.; Mardyani, S.; Chan, W. C. W.; Kumacheva, E. *Adv. Mater.* **2006,** *18*, 80.
26. Soppimath, K. S.; Tan, D. C. W.; Yang, Y. *Adv. Mater.* **2005,** *17*, 318.
27. Kawaguchi, H.; Fujimoto, K. *Bioseparation* **1998,** *7*, 253.
28. Sahiner, N.; Godbey, W. T.; Mcpherson, G. L.; John, V. T. *Colloid Polym. Sci.* **2006,** *284*, 1121.
29. Ivanov, I. E.; Kazakov, S. V.; Yu, I.; Mattiasson, G. B. *Polymer* **2001,** *42*, 3373.
30. Pelton, R. H.; Chibante, P. *Colloids Surf.* **1986,** *20*, 247.
31. Sanghavi, P. G.; Devi, S. *Int. J. Polym. Mater.* **2005,** *54*, 293.
32. Bhawal, S.; Reddy, L. H. V.; Murthy, R. S. R.; Devi, S. *J. Appl. Polym. Sci.* **2004,** *92*, 402.
33. Shah, S. S.; Pal, A.; Rajyaguru, T.; Murthy, R. S. R.; Devi, S. *J. Appl. Polym. Sci.* **2008,** *107*, 3221.
34. Shah, S. S.; Pal, A.; Gude, R. P.; Devi, S. *Eur. Polym. J.* **2010,** *958*, 46.
35. Yan, X.; Gemeinhart, R. A. *J. Controlled Release* **2005,** *106*, 198.
36. Kirsh, Y. E.; Yanula, N. A.; Kalninsh, K. K. *Eur. Polym. J.* **1999,** *35*, 305.
37. Wang, F.; Bronich, T. K.; Kabanov A. V.; Rauh, R. D.; Roovers, J. *Bioconjugate Chem.* **2005,** *16*, 397.
38. Lamprecht, A.; Benoit, J. P. *J Controlled Release* **2006,** *112*, 208.
39. Adams, M. L.; Lavasanifar, A.; Kwon, G. S. *J. Pharm. Sci.* **2003,** *92*, 1343.
40. Jasti, B. R.; Du, J.; Vasavada, R. C. *Int. J. Pharm.* **1995,** *118*, 161.
41. Qiu, X.; Sukhishvili, S. A. *J. Polym. Sci. Part A: Polym. Chem.* **2006,** *44*, 183.